From embedded solitons to 4d dynamical systems

E. Cabrera[a], S. González-Pérez-Sandi, and J. Fujioka[b]
[a]*Departamento de Estado Sólido;* [b]*Departamento de Materia Condensada;*
Instituto de Física, Universidad Nacional Autónoma de México,
04510 México D.F., México.

Recibido el 17 de noviembre de 2006; aceptado el 8 de enero de 2007

The term "embedded soliton" was coined in 1999 to describe a new type of soliton (discovered in 1997) whose internal frequencies lie within the spectrum of the radiation modes of certain nonlinear systems. In 2005 it was discovered that "embedded lattice solitons" (ELS) can also exist in discrete systems. The present communication shows that a discrete higher-order NLS equation with exact ELS leads naturally to a four-dimensional dynamical system that can be cast in the form $\phi_{n+4} = F(\phi_n, \ldots, \phi_{n+3})$, where F is a nonlinear function. In all the particular cases studied in this communication, at least two of the four Lyapunov coefficients associated with the system are positive, thus indicating a chaotic behavior.

Keywords: Embedded solitons; lattice solitons; dynamical systems; discrete NLS equation; nonlinear Schrodinger equation.

En 1997 se decubrió un nuevo tipo de solitones, los cuales fueron bautizados en 1999 con el nombre de "solitones embebidos" (SEs). A diferencia de los solitones normales, los SEs tienen frecuencias internas que están dentro del espectro de los modos de radiación de ciertos sistemas no lineales. Recientemente se descubrió que también existen "solitones embebidos discretos", tanto estables como inestables. En el presente trabajo se muestra que una versión discreta de una ecuación no lineal de Schrodinger generalizada conduce de manera natural a un sistema dinámico no lineal en cuatro dimensiones. Este sistema dinámico genera órbitas sumamente interesantes y de particular belleza. En todos los casos que estudiamos en este trabajo encontramos que al menos dos de los cuatro coeficientes de Lyapunov calculados resultaron ser positivos, sugiriendo así la existencia de soluciones caóticas.

Descriptores: Solitones embebidos; solitones discretos; sistemas dinámicos; ecuación NLS discreta; ecuación no lineal de Schrodinger.

PACS: 05.45.Yv; 05.45.-a; 42.65.Tg

1. Introduction

The discretization of soliton equations leads in a natural way to nonlinear mappings (NMs) with interesting properties. In particular, NMs associated with differential-difference versions of the Korteweg-de Vries (KdV), modified KdV, isotropic Heisenberg spin chain (IHSC) and nonlinear Schrödinger (NLS) equations have been shown to possess interesting structures [1–3]. These equations have, as a common feature, the possession of standard soliton solutions. There exist, however, nonlinear equations with non-standard solitons, which can also lead to interesting NMs. In particular, the present communication focuses on the study of the NMs associated with a novel type of soliton christened in 1999 *as embedded solitons* (ES).

The ES can be described by real or complex functions. When ES are complex, they are characterized by possessing internal frequencies which lie within the range of frequencies permitted for radiation modes. In the case of real ES, the embedded quantity is the velocity of the solitons, which lie among the phase velocities permitted for linear waves. Usually this feature would imply that this type of soliton should decay into radiation, due to a resonance between the soliton and the radiation modes. In fact, *all* standard complex solitons have internal frequencies which lie *outside* the spectrum of the radiation modes in order to avoid this resonance. However, in the case of ES, a delicate balance between nonlinearity and dispersion prevents the resonant emission of radiation, thus permitting the existence of these solitons.

In the beginning ES were only found in continuous systems occurring in nonlinear optics [4–7], hydrodynamics [8] and liquid crystal theory [9]. However, it was recently found that ES can also exist in discrete systems [10,11], and in these cases we speak of *embedded lattice solitons* (ELS).These discrete systems with ELS lead immediately to new NMs which have not been studied previously. In the present communication, we will study the NMs which arise from the first differential-difference equation which was shown to possess *explicit* ELS. This equation is a discrete version of a higher-order nonlinear Schrödinger (NLS) equation:

$$i\frac{\partial u}{\partial t} + \varepsilon_2 \frac{\partial^2 u}{\partial x^2} + \varepsilon_4 \frac{\partial^4 u}{\partial x^4} + \gamma_1 |u|^2 - \gamma_2 |u|^4 u = 0, \quad (1)$$

which is useful in describing the propagation of ultrafast optical pulses in fibers doped with two appropriate materials [12]. In this case t represents the propagation distance, x is the retarded time, ε_n and γ_n are real constants, and $u(x,t)$ is a complex function. In Ref. 10 it was shown that a discrete version of (1) which has ELS has the form:

$$i\frac{\partial r_n}{\partial t} + \varepsilon_2 \triangle_2 r_n + \varepsilon_4 \triangle_4 r_n + \frac{1}{2}\gamma_1 |r_n|^2 (r_{n+1} + r_{n-1}) - \frac{2}{3}\gamma_2 |r_n|^4 [r_{n+2} + 4\alpha (r_{n+1} + r_{n-1}) + r_{n-2}] = 0, \quad (2)$$

where $r_n(t) = u(n\Delta x, t)$ is a complex-valued function of time defined at the lattice sites, the coefficients ε_n, γ_n and α

are real, and the finite-difference operators Δ_2 and Δ_4 are:

$$\Delta_2\ r_n \equiv \frac{r_{n+1} - 2\,r_n + r_{n-1}}{(\Delta x)^2}, \tag{3}$$

$$\Delta_4\ r_n \equiv \frac{r_{n+2} - 4\,r_{n+1} + 6\,r_n - 4\,r_{n-1} + r_{n-2}}{(\Delta x)^4}, \tag{4}$$

where Δx is the lattice spacing. An interesting feature of Eq. (2) is that it not only involves the nearest neighboring interactions, but also the next-nearest contributions, and this feature implies that the NMs associated with this equation will be four-dimensional (4D).

The soliton solutions of Eq. (2) are particular solutions of the form:

$$r_n(t) = \phi_n e^{-i\omega\,t}, \tag{5}$$

where $\phi_n = A\,\mathrm{sech}(B\,n\,\triangle x)$, and the values of the constants A, B and ω can be found from a complex system of algebraic equations. These soliton solutions were studied elsewhere [10], and in the present communication we will focus our attention on other solutions of the form (5). Substituting (5) into (2) it is easily found that ϕ_n must satisfy the following equation:

$$\begin{aligned}\phi_{n+4} = &[(\omega - 2\,\varepsilon_2^o + 6\,\varepsilon_4^o)\,\phi_{n+2} \\ &+ \left(\varepsilon_2^o - 4\,\varepsilon_4^o + \gamma_1^o\phi_{n+2}^2 - 4\alpha\gamma_2^o\,\phi_{n+2}^4\right)(\phi_{n+3} + \phi_{n+1}) \\ &+ \left(\varepsilon_4^o - \gamma_2^o\phi_{n+2}^4\right)\phi_n] * \left(\gamma_2^o\,\phi_{n+2}^4 - \varepsilon_4^o\right)^{-1},\end{aligned} \tag{6}$$

where:

$$\varepsilon_2^o{=}\frac{\varepsilon_2}{(\Delta x)^2}, \quad \varepsilon_4^o{=}\frac{\varepsilon_4}{(\Delta x)^4}, \quad \gamma_1^o{=}\frac{\gamma_1}{2}, \quad \gamma_2^o{=}\frac{2}{3}\gamma_2. \tag{7}$$

Equation (8) can be rewritten as the following first-order system in a 4D space, with $a_n = \phi_n$:

$$a_{n+1} = b_n, \tag{8}$$

$$b_{n+1} = c_n, \tag{9}$$

$$c_{n+1} = d_n, \tag{10}$$

$$\begin{aligned}d_{n+1} = &[(\omega - 2\,\varepsilon_2^o + 6\,\varepsilon_4^o)\,c_n \\ &+ \left(\varepsilon_2^o - 4\,\varepsilon_4^o + \gamma_1^o c_n^2 - 4\alpha\gamma_2^o\,c_n^4\right)(d_n + b_n) \\ &+ \left(\varepsilon_4^o - \gamma_2^o c_n^4\right)a_n] * \left(\gamma_2^o c_n^4 - \varepsilon_4^o\right)^{-1}.\end{aligned} \tag{11}$$

In the present communication we shall explore the rich variety of solutions of this 4D dynamical system. In Sec. 2 we shall calculate the fixed points of this system in two different cases ($\omega = 0$ and $\omega \neq 0$), and the behavior of the solutions close to and far away from these points will be investigated. Then, in Sec. 3, we shall study what is the influence of the coefficients α, ε_n^o, γ_n^o and ω on the solution of the system (8)-(11). Finally, Sec. 4 concludes the paper.

2. Behavior close to and far away from the fixed points

2.1. Fixed points

To simplify the notation, let us rewrite the system (8)-(11) in the compact form:

$$\mathbf{x}_{n+1} = \mathbf{f}\left(\mathbf{x}_n\right), \tag{12}$$

where $\mathbf{x}_n = (a_n, b_n, c_n, d_n) \in \mathbb{R}^4$, and $\mathbf{f} : \mathbb{R}^4 \to \mathbb{R}^4$ is the function:

$$\mathbf{f}\left(\mathbf{x}_n\right) = \left(f_1(\mathbf{x}_n), f_2(\mathbf{x}_n), f_3(\mathbf{x}_n), f_4(\mathbf{x}_n)\right), \tag{13}$$

and $f_i{:}\,\mathbb{R}^4 \to \mathbb{R}$ are defined as follows:

$$f_1\left(a_n, b_n, c_n, d_n\right) = b_n, \tag{14}$$

$$f_2\left(a_n, b_n, c_n, d_n\right) = c_n, \tag{15}$$

$$f_3\left(a_n, b_n, c_n, d_n\right) = d_n, \tag{16}$$

$$\begin{aligned}f_4\left(a_n, b_n, c_n, d_n\right) = &[(\omega - 2\,\varepsilon_2^o + 6\,\varepsilon_4^o)\,c_n \\ &+ \left(\varepsilon_2^o - 4\,\varepsilon_4^o + \gamma_1^o c_n^2 - 4\alpha\gamma_2^o\,c_n^4\right)(d_n + b_n) \\ &+ \left(\varepsilon_4^o - \gamma_2^o c_n^4\right)a_n] * \left(\gamma_2^o c_n^4 - \varepsilon_4^o\right)^{-1}.\end{aligned} \tag{17}$$

Now let us find the fixed points of system (12). These points are the solutions to the equation $\mathbf{x} = \mathbf{f}\left(\mathbf{x}\right)$, and from this equation it follows that these points have the form $\mathbf{x} = (p, p, p, p)$, where p is any of the real roots of the equation:

$$2(4\alpha + 1)\gamma_2^o\,p^5 - 2\gamma_1^o\,p^3 - \omega p = 0. \tag{18}$$

This equation may have one, three or five roots, depending on the values of the coefficients γ_1^o, γ_2^o, α and ω. One of these roots is $p_1 = 0$ [which is associated with the soliton solutions to Eq. (2)], and the remaining four roots (when they exist) are defined by the equations:

$$p_{2,3} = \pm\sqrt{\frac{4\gamma_1^o + \sqrt{4(\gamma_1^o)^2 + 8\gamma_2^o\omega(4\alpha+1)}}{8\gamma_2^o(4\alpha+1)}}, \tag{19}$$

$$p_{4,5} = \pm\sqrt{\frac{4\gamma_1^o - \sqrt{4(\gamma_1^o)^2 + 8\gamma_2^o\omega(4\alpha+1)}}{8\gamma_2^o(4\alpha+1)}}. \tag{20}$$

To determine the stability of each of these fixed points, we need the eigenvalues of the equation:

$$Det\left[\mathbf{R} - \lambda\mathbf{I}\right] = 0, \tag{21}$$

where $\mathbf{I}$ is the identity matrix and $\mathbf{R}$ is the jacobian of the system (12), which has the form:

$$\mathbf{R} = \begin{bmatrix} 0 & 1 & 0 & 0 \\ 0 & 0 & 1 & 0 \\ 0 & 0 & 0 & 1 \\ -1 & s & t & s \end{bmatrix}, \tag{22}$$

where s and t depend on γ_1^o, γ_2^o, α, ω and p in the following way:

$$s = \frac{\varepsilon_2^o - 4\varepsilon_4^o + \gamma_1^o\, p^2 - 4\alpha\gamma_2^o\, p^4}{\gamma_2^o\, p^4 - \varepsilon_4^o}, \tag{23}$$

$$\begin{aligned} t = \left(\gamma_2^o\, p^4 - \varepsilon_4^o\right)^{-2} \big[&- \left(\omega - 2\varepsilon_2^o + 6\varepsilon_4^o\right)\left(\varepsilon_4^o + 3\gamma_2^o\, p^4\right) \\ &- 2p^2 \left\{4\gamma_2^o\, \varepsilon_2^o\, p^2 + 2\gamma_1^o \left(\gamma_2^o\, p^4 + \varepsilon_4^o\right)\right. \\ &\left. -16\gamma_2^o\, \varepsilon_4^o \left(\alpha + 1\right)\, p^2\right\}\big]. \end{aligned} \tag{24}$$

From Eqs. (21) and (22), it follows that the four eigenvalues are the roots of the equation:

$$\lambda^4 - s\lambda^3 - t\lambda^2 - s\lambda + 1 = 0. \tag{25}$$

Once these values are known, the stability of each of the fixed points is determined by the norm of the matrix $\mathbf{R}$, which is defined as:

$$||\mathbf{R}|| = \max\left\{|\lambda_1|, |\lambda_2|, |\lambda_3|, |\lambda_4|\right\}. \tag{26}$$

The fixed point will be stable if $||\mathbf{R}|| \langle 1$, unstable if $||\mathbf{R}|| \rangle 1$, and the stability of the point remains undefined if $||\mathbf{R}|| = 1$.

We shall now study the behavior of the system (12) close to and far away from the fixed points in two different cases defined by the parameters shown in Table I.

In Case 2, the parameters ε_2, ε_4, γ_1, γ_2, Δx, α and ω were chosen in order for Eq. (2) to have ELS. On the other hand, in Case 1 the mapping (8)-(11) is simpler because $\omega = 0$, but in this case Eq. (2) has no ELS.

As we shall see below, interesting patterns are obtained in the phase plane (ϕ_n, ϕ_{n+1}) when the sequence of values $\{\phi_n\}$ is obtained by means of Eq. (6). The nature of these patterns (periodic, quasiperiodic, chaotic, etc.) will be analyzed by calculating the fast Fourier transform (FFT) and the Lyapunov exponents corresponding to these sequences $\{\phi_n\}$. As Eq. (6) defines a fourth-order dynamical system, there will be four Lyapunov exponents, which we will calculate by means of the procedure explained in Refs. 13 and 14.

TABLE I. Parameters used in the cases studied.

	Case 1	Case 2
ε_2	1	1
ε_4	$24/49$	$24/49$
γ_1	1	1
γ_2	1	1
Δx	1	1
α	-0.066599269	-0.066599269
ω	0	-0.212026829

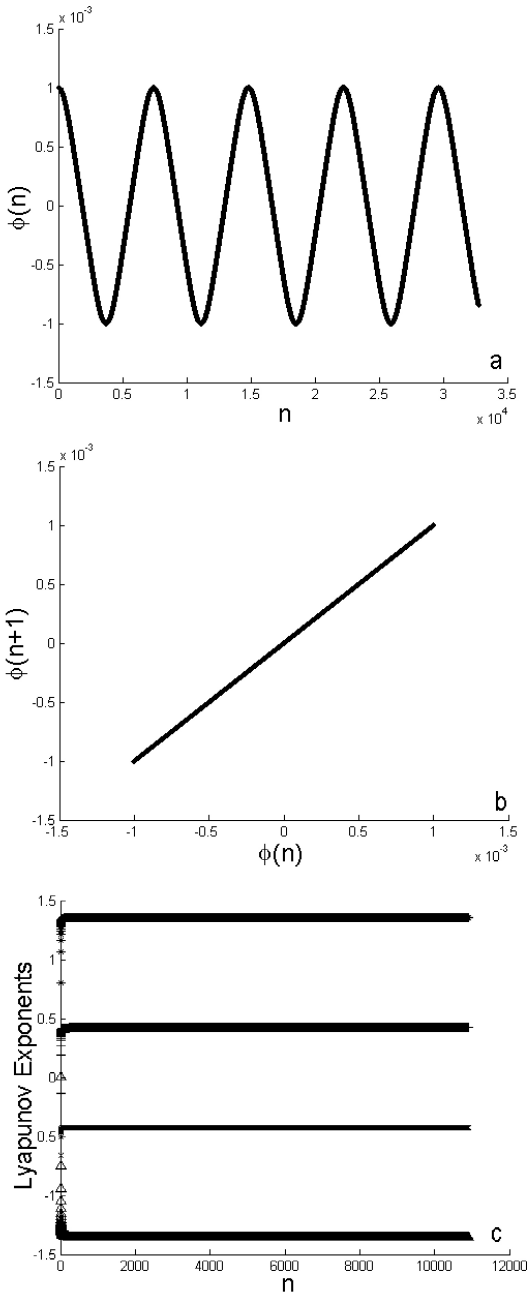

FIGURE 1. Solution corresponding to Case 1 ($\omega = 0$) with the initial condition $a_0 = b_0 = c_0 = d_0 = 0.001$, which is close to the fixed point $\mathbf{x}^{(1)}$. (a) Values of ϕ_n for $n = 0, ...32767$, (b) phase portrait of the points (ϕ_n, ϕ_{n+1}), (c) Lyapunov exponents.

2.2. Case 1 $(\omega = 0)$

In this case, system (12) has three fixed points:

$$\mathbf{x}^{(1)} = (0, 0, 0, 0)$$

$$\mathbf{x}^{(2)} = (p_2, p_2, p_2, p_2)\,; \qquad p_2 = +1.011114$$

$$\mathbf{x}^{(3)} = (p_3, p_3, p_3, p_3)\,; \qquad p_3 = -1.011114.$$

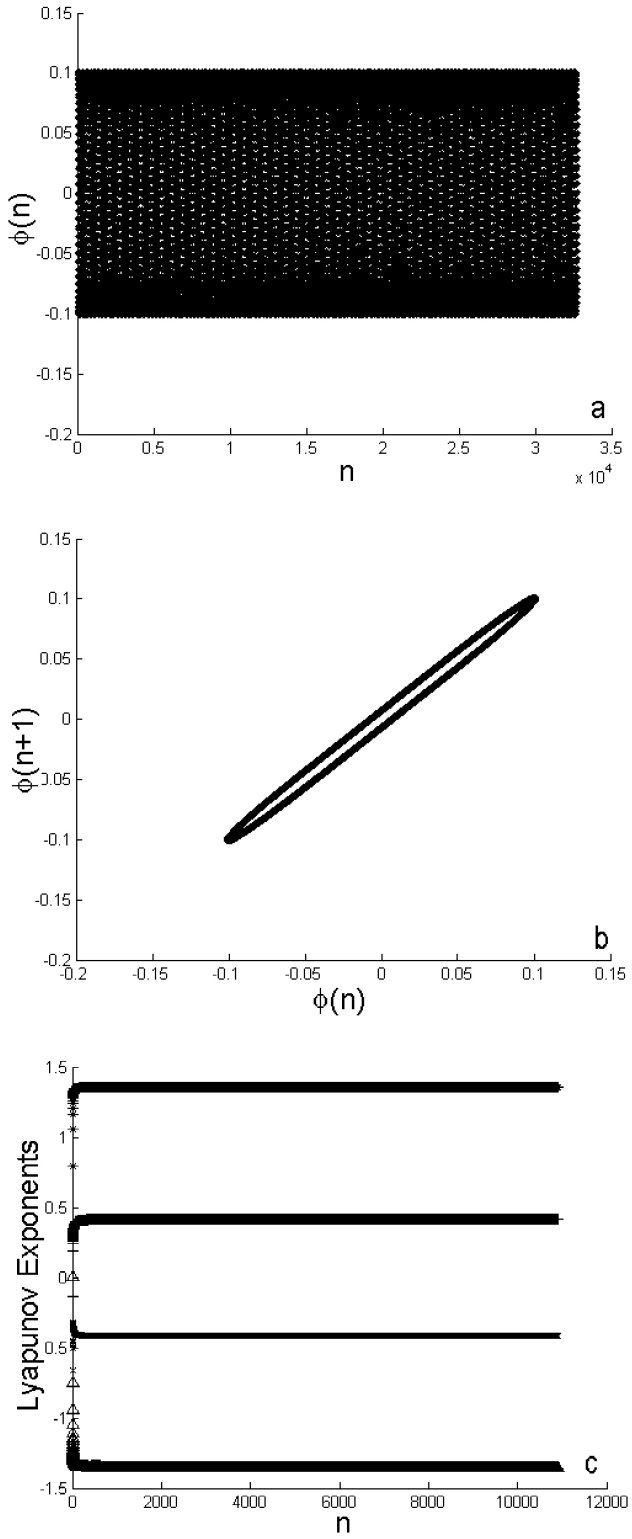

FIGURE 2. Solution corresponding to Case 1 ($\omega = 0$) with the initial condition $a_0 = b_0 = c_0 = d_0 = 0.1$, which is close to the fixed point $\mathbf{x}^{(1)}$. (a) Values of ϕ_n for $n = 0, ..., 32767$, (b) phase portrait of the points (ϕ_n, ϕ_{n+1}), (c) Lyapunov exponents.

The linear stability analysis indicates that points $\mathbf{x}^{(2,3)}$ are unstable, and gives no information concerning point $\mathbf{x}^{(1)}$. The numerical tests show that the behavior of the solutions near point $\mathbf{x}^{(1)}$ is simple. In Fig. 1a, for example, we can see a periodic solution corresponding to the initial condition $a_0 = b_0 = c_0 = d_0 = 0.001$. The phase portrait of this solution in the plane (ϕ_n, ϕ_{n+1}) is trivial, and can be seen in Fig. 1b. Figure 1c shows the Lyapunov exponents associated with this solution. If the initial condition is moved a little bit farther from $\mathbf{x}^{(1)}$, quasiperiodic solutions are obtained. For example, the initial condition $a_0 = b_0 = c_0 = d_0 = 0.1$ leads to the quasiperiodic solution shown in Fig. 2a. The phase portrait and the Lyapunov exponents corresponding to this solution are shown in Figs. 2b and 2c.

The behavior of the solutions near points $\mathbf{x}^{(2,3)}$ is more interesting. In Fig. 3 we can see, for example, the solution corresponding to the initial condition $a_0{=}b_0{=}c_0{=}d_0{=}1.011112$, which is close to $\mathbf{x}^{(2)}$. Fig. 3a shows that the sequence $\{\phi_n\}$ seems to have different sections. In each of these sections the value of $|\phi_n|$ remains bounded, *i.e.*, $|\phi_n| \langle B_n$ within the *n-th* section. The phase portrait corresponding to the movement of the point (ϕ_n, ϕ_{n+1}) is shown in Fig. 3b, and the Fourier transform is presented in Fig. 3c. This solution is quite sensitive to the initial conditions, as shown by the increasing positive Lyapunov exponents shown in Fig. 3d. The different sections of the sequence $\{\phi_n\}$ seen in Fig. 3a correspond to different quasiperiodic orbits. The "jumps" from one quasiperiodic orbit to another shown in Fig. are spurious, and occur when the denominator of expression (17) comes too close zero and the computer is not enough to evaluate the quotient accurately enough. Therefore, the position of the jumps changes if we increase the computers precision.

Far from the fixed points, the solutions behave similarly to the solution shown in Fig. 3. In Fig. 4, for example, we can see the behavior of the solution corresponding to the initial condition $a_0 = c_0 = 1.394$ and $b_0 = d_0 = 1.393$. Figure 4a shows that the solution also seems to evolve by steps. However, as in Fig. 3, the jump from one step to the next is a spurious result due to the finite accuracy of the computer. The phase portrait of the solution is shown in Fig. 4b. We can see two well-defined elliptical structures in this figure. These structures correspond to two of the steps shown in Fig. 4a. In Fig. 4c we can see that the FFT of this solution exhibits four well-defined wavenumbers (± 2.267 and $\pm\, 0.677$), which are associated with elliptical rings seen in Fig. 4b. This solution is also rather sensitive to the initial conditions, as shown by the Lyapunov exponents shown in Fig. 4d.

2.3. Case 2 ($\omega \neq 0$)

Now let us consider Case 2. In this case, system (12) has five fixed points:

$$\mathbf{x}^{(1)} = (0, 0, 0, 0)\,,$$

$$\mathbf{x}^{(2,3)} = \pm\,(p_2, p_2, p_2, p_2)\,; \qquad p_2 = 0.547853$$

$$\mathbf{x}^{(4,5)} = \pm\,(p_4, p_4, p_4, p_4)\,; \qquad p_4 = 0.849828$$

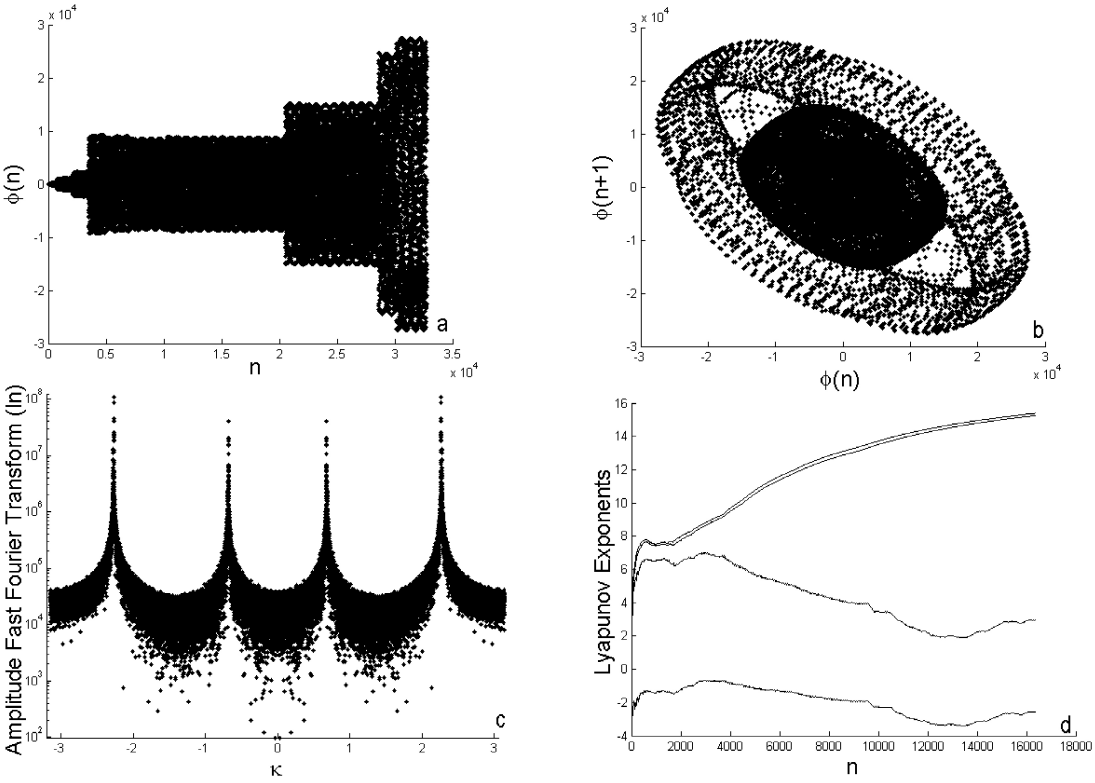

FIGURE 3. Solution corresponding to Case 1 ($\omega = 0$) with the initial condition $a_0 = b_0 = c_0 = d_0 = 1.011112$, which is close to the fixed point $\mathbf{x}^{(2)}$. (a) Values of ϕ_n for $n = 0, ...32767$, (b) phase portrait of the points (ϕ_n, ϕ_{n+1}), (c) Fourier transform, (d) Lyapunov exponents.

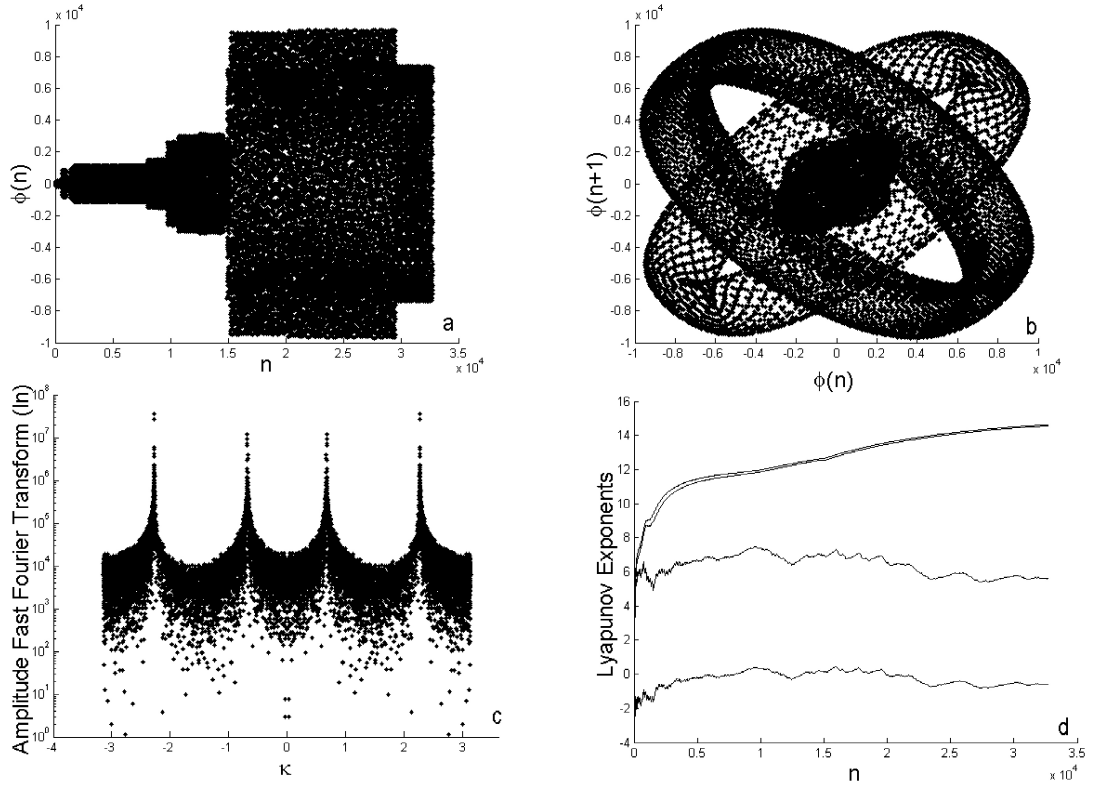

FIGURE 4. Solution corresponding to Case 1 ($\omega = 0$) with the initial condition $a_0 = c_0 = 1.394\ and\ b_0 = d_0 = 1.393$, which is far from the fixed points. (a) Values of ϕ_n for $n = 0, ..., 32767$, (b) phase portrait of the points (ϕ_n, ϕ_{n+1}), (c) Fourier transform, (d) Lyapunov exponents.

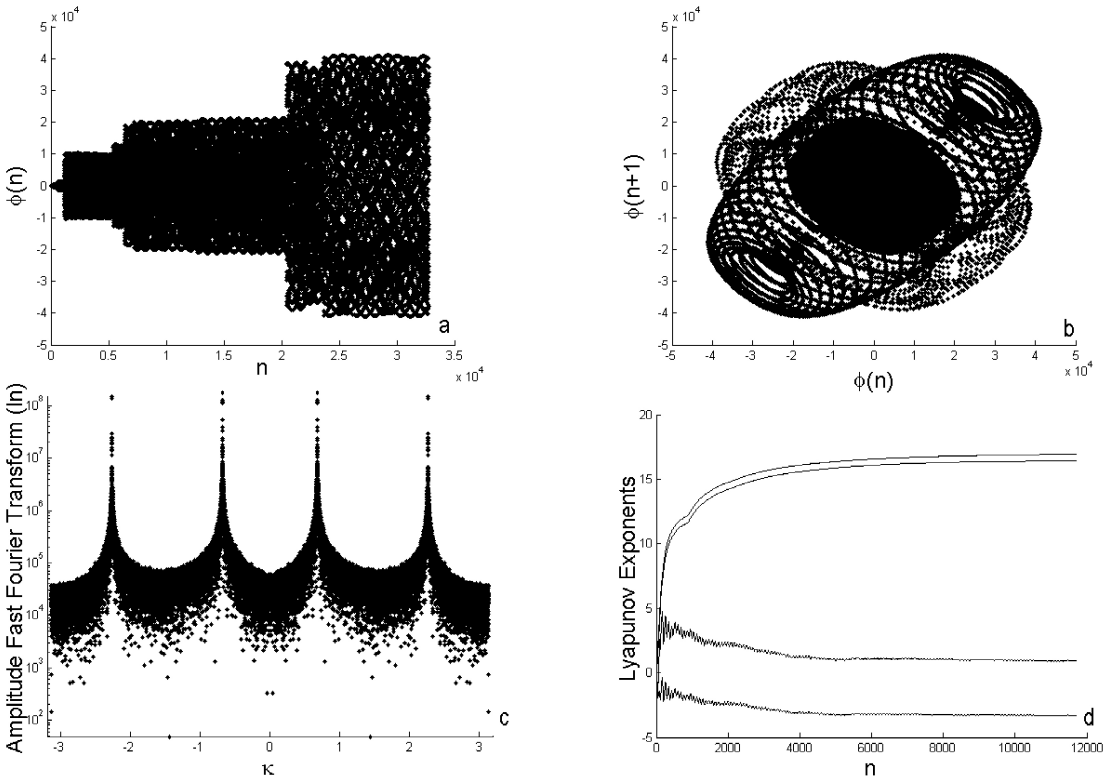

FIGURE 5. Solution corresponding to Case 2 ($\omega \neq 0$) with the initial condition $a_0 = b_0 = c_0 = d_0 = 0.001$, which is close to the fixed point $\mathbf{x}^{(1)}$. (a) Values of ϕ_n for $n = 0, ...32767$, (b) phase portrait of the points (ϕ_n, ϕ_{n+1}), (c) Fourier transform, (d) Lyapunov exponents.

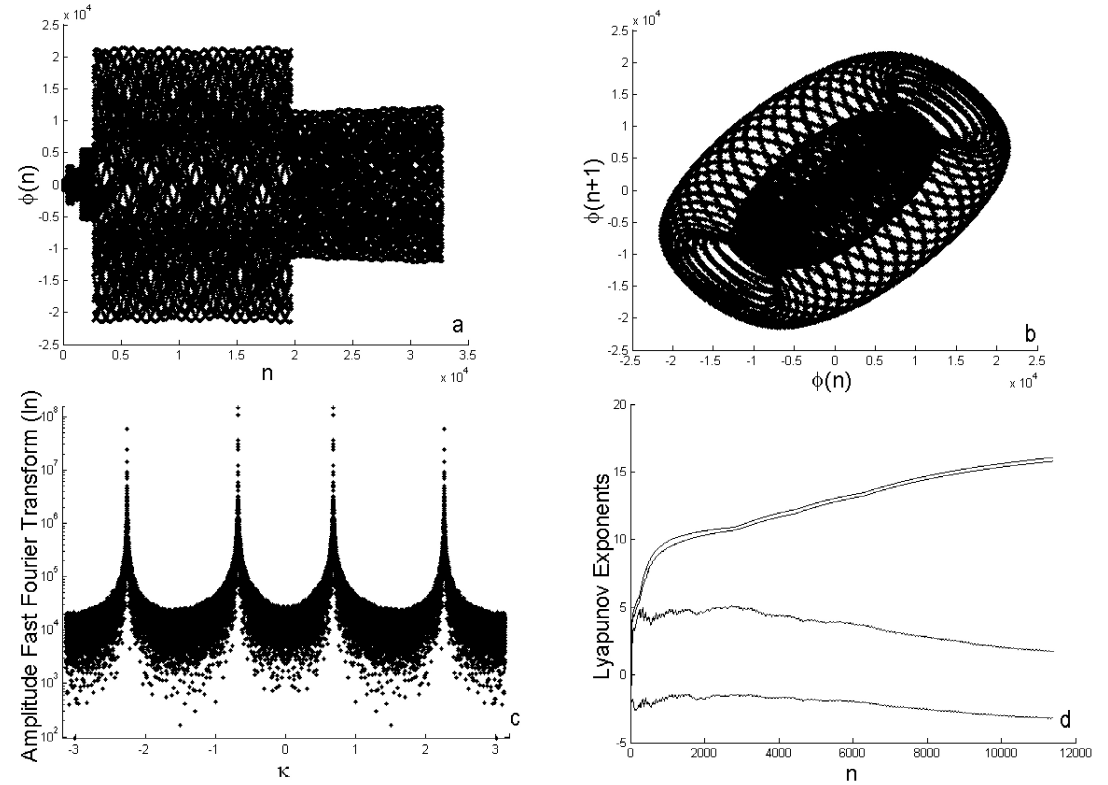

FIGURE 6. Solution corresponding to Case 2 ($\omega \neq 0$) with the initial condition $a_0 = b_0 = c_0 = d_0 =$0.85, which is close to the fixed point $\mathbf{x}^{(4)}$.(a) Values of ϕ_n for $n = 0, ...32767$, (b) phase portrait of the points (ϕ_n, ϕ_{n+1}), (c) Fourier transform, (d) Lyapunov exponents.

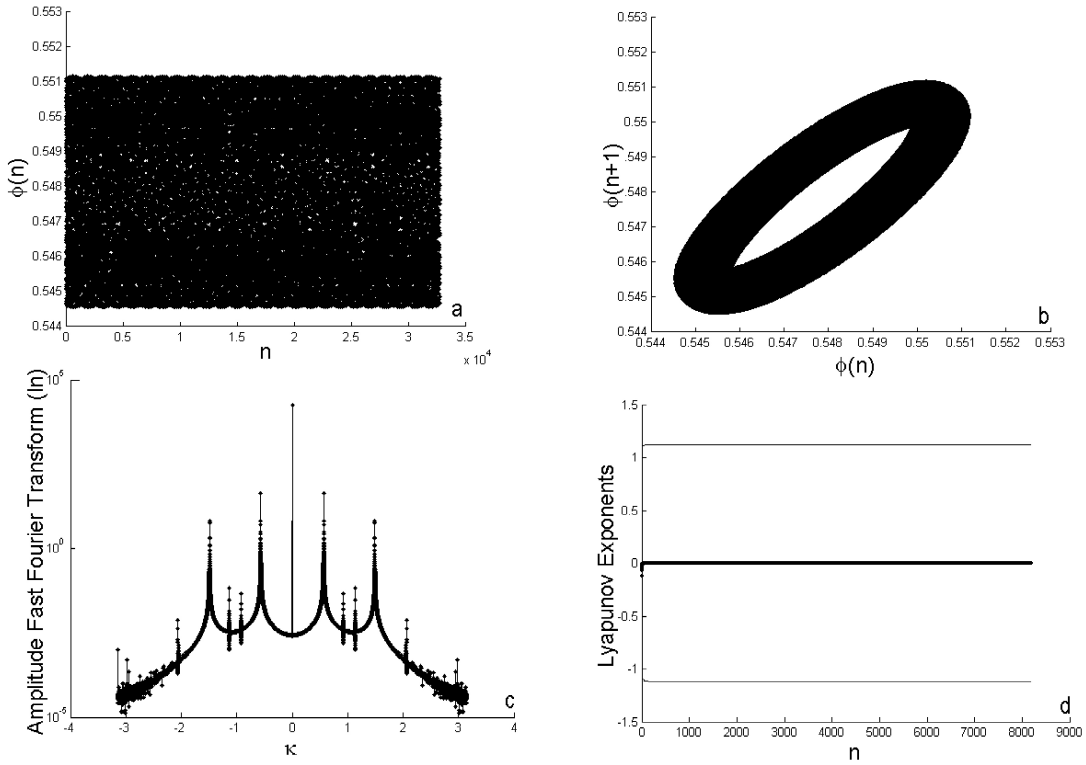

FIGURE 7. Solution corresponding to Case 2 ($\omega \neq 0$) with the initial condition $a_0 = b_0 = c_0 = d_0 = 0.55$, which is close to the fixed point $\mathbf{x}^{(2)}$. (a) Values of ϕ_n for $n = 0, ..., 32767$, (b) phase portrait of the points (ϕ_n, ϕ_{n+1}), (c) Fourier transform, (d) Lyapunov exponents.

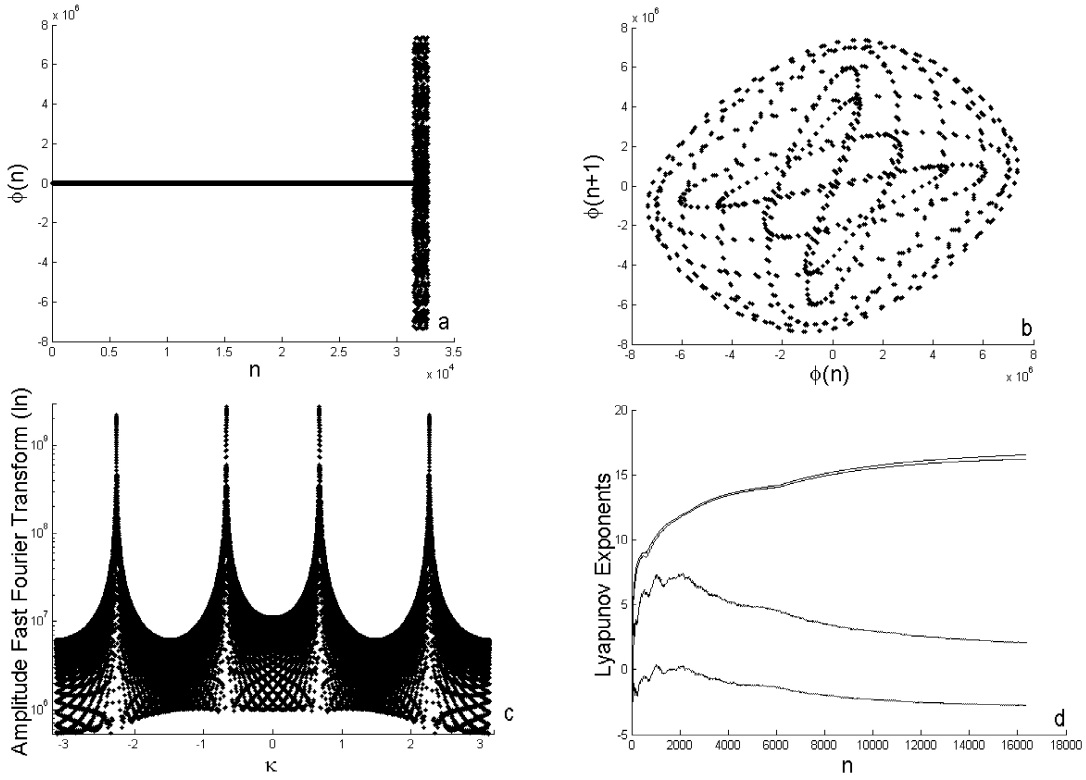

FIGURE 8. Solution corresponding to Case 2 ($\omega \neq 0$) with the initial condition $a_0 = c_0 = 0.25$ and $b_0 = d_0 = 0.3$, which is far from the fixed points. (a) Values of ϕ_n for $n = 0, ..., 32767$, (b) phase portrait of the points (ϕ_n, ϕ_{n+1}), (c) Fourier transform, (d) Lyapunov exponents.

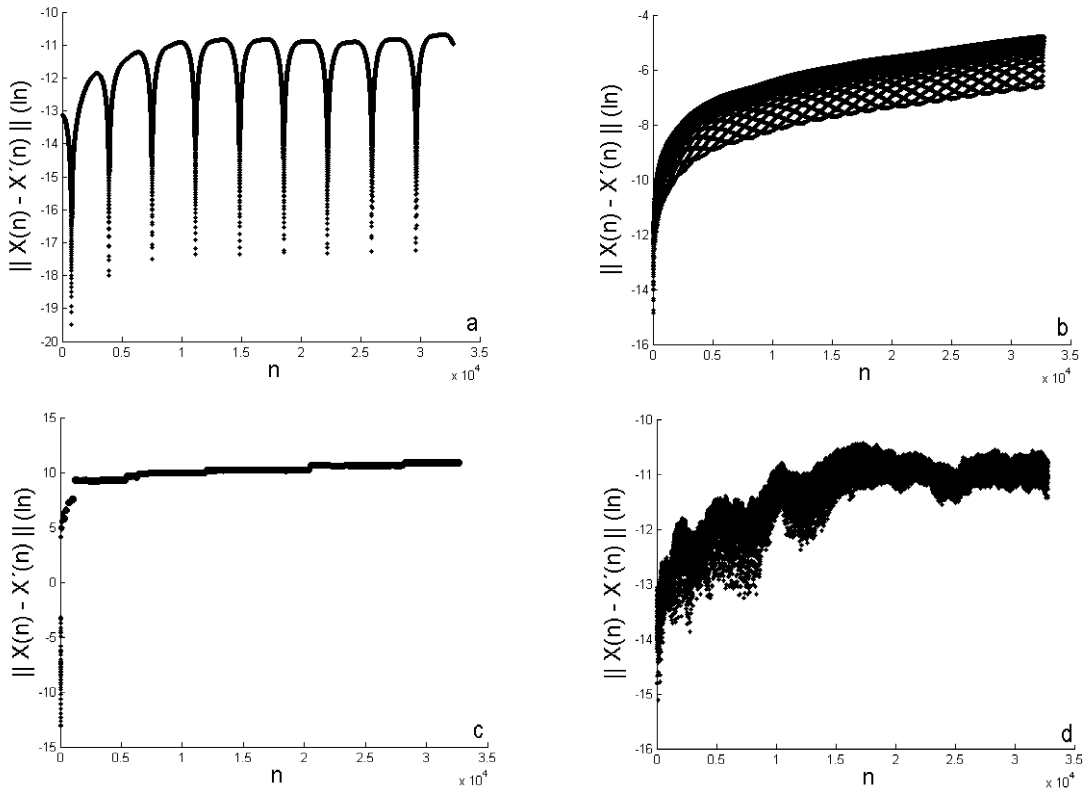

FIGURE 9. Influence of a small change in the initial conditions which leads to Figs. 1, 2, 7 and 8. A small change ($\Delta\phi = 10^{-6}$) was added to the initial conditions which produced these figures, and the distances between the initial and the modified solutions are shown on the vertical axes of the graphs (a), (b), (c) and (d) shown above.

The linear stability analysis shows that point $\mathbf{x}^{(1)}$ is unstable (as expected, since this point is associated with soliton solution), the stability of points $\mathbf{x}^{(2,3)}$ remains undefined, and points $\mathbf{x}^{(4,5)}$ are also unstable. The behavior of the solutions near these points can be seen in Figs. 5-7.

The graphs shown in Figs. 5a and 6a show that the upper bound of the solutions whose initial conditions are close to the unstable fixed points $\mathbf{x}^{(1)}$ and $\mathbf{x}^{(4)}$ also change by steps [in a form similar to the solution shown in Fig. 4a]. The Fourier transforms shown in Figs. 5c and 6c present four dominant wavenumbers [± 0.681 and ± 2.270 in case 5c, and ± 0.681 and ± 2.270 in case 6c]. The Lyapunov exponents shown in Figs. 5d and 6d indicate that the solutions are also sensitive to initial conditions in these two cases.

In Figs. 7a and 7b, we can see a quasiperiodic solution whose initial condition is close to point $\mathbf{x}^{(2)}$. The Fourier transform presented in Fig. 7c shows that there are 12 dominant wavenumbers. Fig. 7d shows that the Lyapunov exponents are almost constant, and one of them is clearly greater than zero, indicating that the solution is sensitive to the initial conditions.

Far from the fixed points, the solutions are more complex. In Fig. 8, for example, we can see the solution corresponding to coefficients $\varepsilon_2^o = 1$, $\varepsilon_4^o = 24/49$, $\gamma_1^o = 0.468750$, $\gamma_2^o = 0.640625$, $\alpha = -0.07$ and $\omega = -0.212027$. With these coefficients, there are five fixed points $\mathbf{x} = (p, p, p, p)$ defined by $p = 0, \pm 0.672308, \pm 0.751173$. If we consider the initial condition, $a_0 = 0.25$, $b_0 = 0.3$, $c_0 = 0.25$ and $d_0 = 0.3$ (which is far from the fixed points), the solution behaves as shown in Figs. 8a and 8b. The dominant wavenumbers can be seen in Fig. 8c, and the Lyapunov exponents are shown in Fig. 8d.

2.4. Sensitivity to initial conditions

In all of the examples examined in this section, some of the Lyapunov coefficients turned out to be positive, thus indicating that some of the solutions to the 4D dynamical system (8)-(11) are rather sensitive to the initial conditions. To appreciate how the solution changes when the initial conditions are slightly modified, let us add a tiny increment ($\Delta\phi = 10^{-6}$) to the initial conditions which produced the results shown in Figs. 1, 2, 7 and 8.

To measure the "distance" $\|X - X'\|$ between the original ("old") solution (X) and the "new" solution (X') corresponding to the modified initial condition, we shall consider the following measure:

$$\|X(n) - X'(n)\| = \Big((\phi(n) - \phi'(n))^2 + (\phi(n+1) - \phi'(n+1))^2 + (\phi(n+2) - \phi'(n+2))^2 + (\phi(n+3) - \phi'(n+3))^2 \Big)^{1/2} \quad (27)$$

The effect of the small variation in the initial conditions leading to Figs. 1, 2, 7 and 8 can be seen in Fig. 9. Notice that, on the vertical axis of the graphs shown in this figure, we have *the logarithm* of the distance between the "old" solution and the "new" solution (*i.e.* the solution corresponding to the modified initial condition). The graphs shown in Figs. 9a and 9b indicate that in these cases the distances between the old and new solutions oscillate, but remain small. These results show that these solutions are very stable, which is in agreement with the small Lyapunov exponents seen in Figs. 1c and 2d. In the case of Fig. 9c, the distance increases rapidly, but the small Lyapunov exponents seen in Fig. 7d do not indicate a chaotic behavior. In the case of Fig. 9d, the distance remains small but changes erratically. This erratic (chaotic) behavior explains the high positive Lyapunov exponents seen in Fig. 8d.

3. Influence of the coefficients

If we observe the form of the dynamical system (6), it is not evident what the influence is of each of the coefficients $\{\varepsilon_n^o, \gamma_n^o, \alpha, \omega\}$ on the form of the solution $\{\phi_n\}$. In order to clarify this issue, let us vary the values of these coefficients one by one to see how these changes affect the solution $\{\phi_n\}$.

In order to appreciate the influence of ε_2^o, Fig. 10 shows the evolution of ϕ_n when $\varepsilon_2^o = 0$, the remaining coefficients of Eq. (6) are the same as in Case 1 (see Table I), and the initial condition is close to the point $\mathbf{x}^{(1)} = (0,0,0,0)$, which behaves as a stable critial point, as we saw earlier. The result depicted in Fig. 10 shows that ϕ_n grows extremely fast if $\varepsilon_2^o = 0$, thus indicating that the coefficient ε_2^o has a stabilizing influence on the solution $\{\phi_n\}$.

A similar result is obtained if we take $\varepsilon_4^o = 0$. As shown in Fig. 11, the values of ϕ_n also become very large when $\varepsilon_4^o = 0$, thus implying that ε_4^o also helps to stabilize the solution $\{\phi_n\}$.

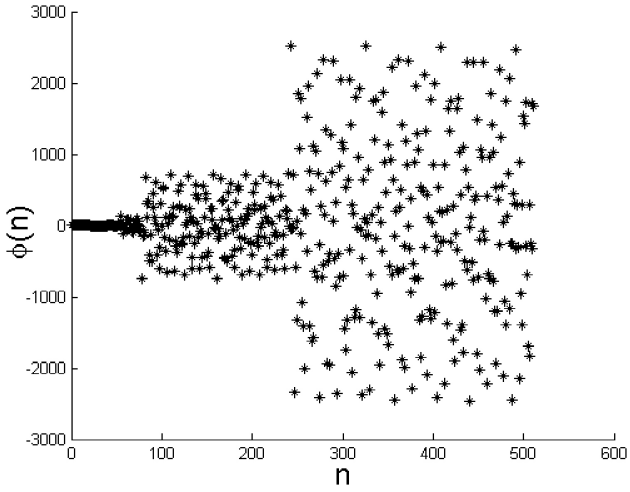

FIGURE 10. Solution corresponding to ε_2^o=0 and the remaining coefficients as in Case 1. The initial condition is: $-\phi(0) = \phi(1) = \phi(2) = \phi(3) = 0.01$.

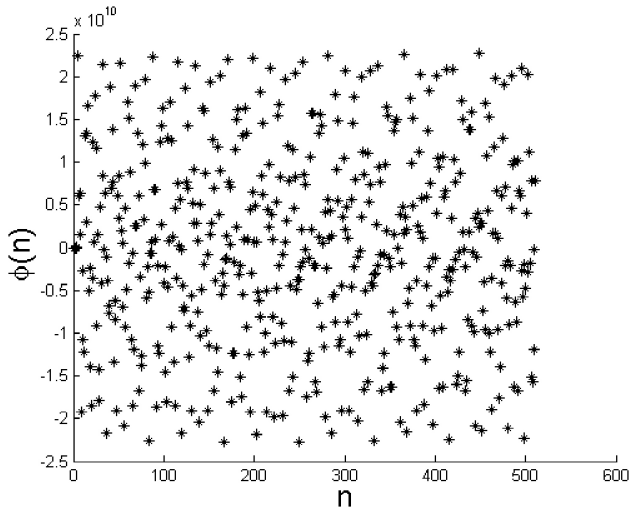

FIGURE 11. Solution corresponding to ε_4^o=0 and the remaining coefficients as in Case 1. The initial condition is: $-\phi(0) = \phi(1) = \phi(2) = \phi(3) = 0.01$.

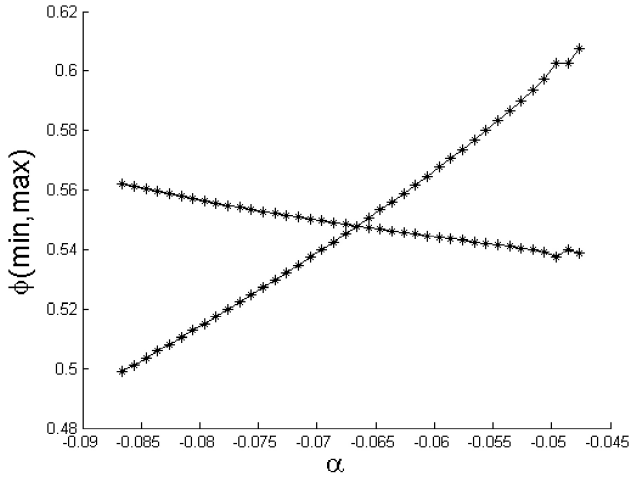

FIGURE 12. Minimum and maximum values of the set $\{\phi_n : n = 0, ..., 2^{14}\}$. Except for α, the parameters as those of Case 2, and the initial condition is the fixed point $\mathbf{x}^{(2)}$.

The effect of α on the solution $\{\phi_n\}$ reveals itself if we plot the minimum and maximum values taken on by ϕ_n during a fixed number (N) of iterations, as functions of α. If we take the parameters corresponding to Case 2 (Table 1), as the initial condition the fixed point $\mathbf{x}^{(2)}$ and $N = 2^{14}$, we arrive at Fig. 12. This figure shows that the range of values spanned by ϕ_n during a fixed number of iterations is a linear function of α (for small variations of α); an interesting result, since α occurs within one of the nonlinear terms of Eq. (2).

The influence of the nonlinear coefficients γ_1^o and γ_2^o is more complicated. In Fig. 13 we can see the minumum and maximum values attained by ϕ_n during $N = 2^{14}$ iterations, as a function of γ_2^o. The initial condition used was the fixed point $\mathbf{x}^{(2)}$ in Case 2, and the remaining coefficients were those of Case 2. As we can see in this figure, the range of values spanned by ϕ_n varies linearly with γ_2^o for small changes in this coefficient, but it increases greatly for $\gamma_2^o > 0.7$ or

$\gamma_2^o < 0.55$. In particular, for $\gamma_2^o > 0.7$, the dependence of this range on γ_2^o seems to be quite irregular and unpredictable.

The effect of γ_1^o is similar. In Fig. 14 we can see that the range of values spanned by ϕ_n varies linearly with γ_1^o for small changes in this coefficient, but it may increase greatly if the value of γ_1^o drops below 0.45. As in Fig. 13, the initial condition used to generate Fig. 14 was the fixed point $\mathbf{x}^{(2)}$ of Case 2, $N = 2^{14}$, and the other parameters were those in Case 2.

The graphs shown in Figs. 13 and 14 reveal that the overall dependence of the range of values spanned by ϕ_n on the coefficients γ_1^o and γ_2^o is complicated and irregular, but this dependence becomes linear for small changes in these two coefficients.

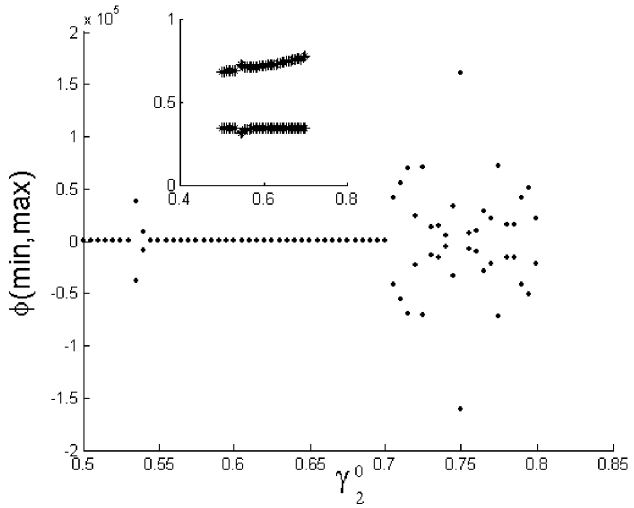

FIGURE 13. Minimum and maximum values of the set $\{\phi_n : n = 0, ..., 2^{14}\}$. Except for γ_2, the parameters are those of Case 2, and the initial condition is the fixed point $\mathbf{x}^{(2)}$.

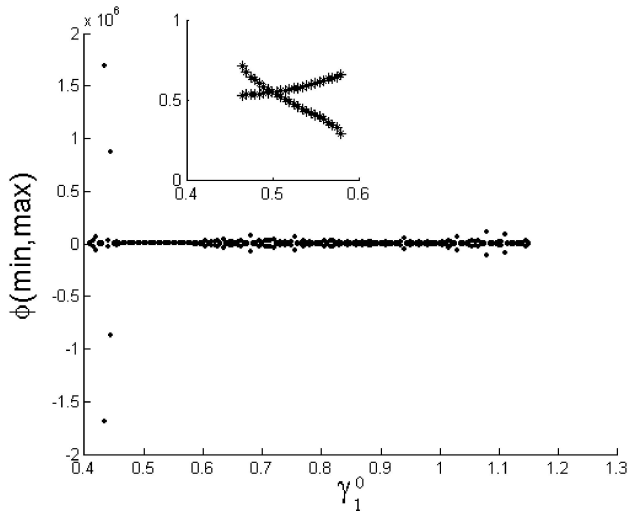

FIGURE 14. Minimum and maximum values of the set $\{\phi_n : n = 0, ..., 2^{14}\}$. Except for γ_1, the parameters are those of Case 2, and the initial condition is the fixed point $\mathbf{x}^{(2)}$.

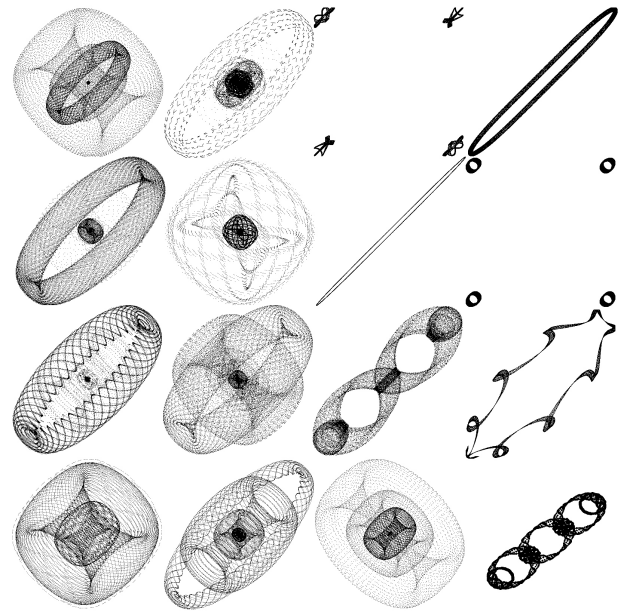

FIGURE 15. Examples of the different types of trajectories which can be generated in the phase plane (ϕ_n, ϕ_{n+1}) when ϕ_n evolves according to Eq. (6). Different coefficients and /or initial conditions were considered to generate these graphs.

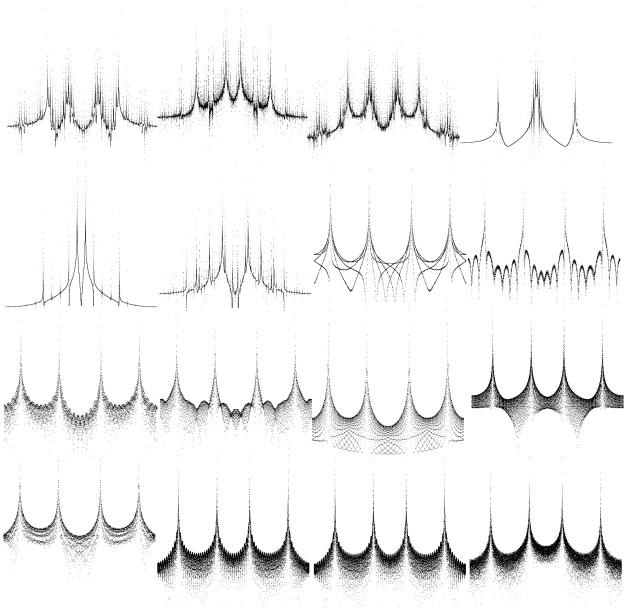

FIGURE 16. Examples of Fourier transforms corresponding to different initial conditions.

4. Discussion and conclusions

In this paper, we have studied the behavior of some of solutions of the nonlinear mapping (6), which is equivalent to the 4D dynamical system (8)-(11). This system is obtained by substituting a separable solution of the form (5) into the nonlinear differential-difference Eq. (2), which is a discrete version of the generalized NLS equation (1). The interest on the solutions of Eq. (2) arises from the fact that this is one

of the two unique systems known to date that possess *explicit* and exact embedded lattice solitons [10–14].

The behavior of ϕ_n [governed by the NM (6)] corresponding to initial conditions close to an unstable fixed point, or far from the fixed points, leads to interesting trajectories in the phase plane (ϕ_n, ϕ_{n+1}), as can be seen in Figs. 3-8. Many other types of trajectories can be obtained by changing the coefficients of the equation, or the initial conditions. In Fig. 15 we can see some examples of the rich variety of trajectories generated in this way.

The evaluation of the four Lyapunov exponents associated with the trajectories in 4D space of a point whose coordinates (a_n, b_n, c_n, d_n) evolve according to the 4D dynamical system (8)-(11) shows that two of these coefficients (and in many cases three of them) are positive, thus implying that the system is chaotic. However, quasiperiodic orbits are possible, as shown by the phase portraits shown in Figs. 3-8 and 15. In these cases, there are four dominating wavenumbers which appear in the Fourier transforms shown in Figs. 3-8. For other initial conditions, different from the ones used to generate Figs. 3-8, the Fourier transforms may be more complicated. In Fig. 16, for example, we can see the structure of the Fourier transforms associated with other initial conditions.

The numerical results indicate that the sequences of values $\{\phi_n\}$ are very sensitive to changes in the nonlinear coefficients γ_1^o and γ_2^o. The effect of changing the linear coefficients ε_2^o and ε_4^o is less dramatic.

1. K.A. Ross and C.J. Thompson, *Physica A* **135** (1986) 551.
2. G.R.W. Quispel, J.A.G. Roberts, and C.J. Thompson, *Phys. Lett. A* **126** (1988) 419.
3. G.R.W. Quispel, J.A.G. Roberts, and C.J. Thompson, *Physica D* **34** (1989) 183.
4. J. Yang, B.A. Malomed, and D.J. Kaup, *Phys. Rev. Lett.* **83** (1999) 1958.
5. A.R. Champneys and B.A. Malomed, *Phys. Rev. E* **61** (2000) 886.
6. A.R. Champneys, B.A. Malomed, J. Yang, and D.J. Kaup, *Physica D* **152-153** (2001) 340.
7. A. Espinosa-Cerón, J. Fujioka, and A. Gómez-Rodríguez, *Physica Scripta* **67** (2003) 314.
8. J. Yang, *Studies in Applied Mathematics* **106** (2001) 337.
9. R.F. Rodríguez, J.A. Reyes, A. Espinosa-Cerón, J. Fujioka, and B.A. Malomed, *Phys. Rev. E* **68** (2003) 036606-1/14.
10. S. González-Pérz-Sandi, J. Fujioka, and B.A. Malomed, *Physica D* **197** (2004) 86.
11. B.A. Malomed, J. Fujioka, A. Espinosa-Cerón, R.F. Rodríguez, and S. González, *Chaos* **16** (2006) 013112.
12. J. Herrmann, *Opt. Commun.* **87** (1992) 161.
13. A. Wolf, J.B. Swift, H.L. Swinney, and J.A. Vaston, *Physica D* **16** (1985) 285.
14. G.L. Baker and J.P. Gollub, *Chaotic Dynamics an introduction*, 2 edition, Cambridge University Press, USA (1998).